Virologica Sinica 39 (2024) 938–950

Contents lists available at ScienceDirect

Virologica Sinica

journal homepage: www.keaipublishing.com/en/journals/virologica-sinica
www.virosin.org

Research Article

Modulation of the unfolded protein response by white spot syndrome virus via wsv406 targeting BiP to facilitate viral replication

Shihan Chen [a,b], Qiqi Zhong [a,b], Xuzheng Liao [a,b], Haiyang Wang [a,b], Bang Xiao [a,b], Jianguo He [a,b,c], Chaozheng Li [a,b,c,*]

[a] School of Marine Sciences, Sun Yat-sen University, State Key Laboratory of Biocontrol/ Southern Marine Science and Engineering Guangdong Laboratory (Zhuhai), Guangzhou, 510275, China
[b] Guangdong Provincial Key Laboratory of Marine Resources and Coastal Engineering/ Guangdong Provincial Key Laboratory for Aquatic Economic Animals, Sun Yat-sen University, Guangzhou, 510275, China
[c] China-ASEAN Belt and Road Joint Laboratory on Marine Aquaculture Technology, Sun Yat-sen University, Guangzhou, 510275, China

ARTICLE INFO

Keywords:
Shrimp
White spot syndrome virus
Unfolded protein response
wsv406
Binding protein (BiP)

ABSTRACT

Outbreaks of diseases are often linked to environmental stress, which can lead to endoplasmic reticulum (ER) stress and subsequently trigger the unfolded protein response (UPR). The replication of the white spot syndrome virus (WSSV), the most serious pathogen in shrimp aquaculture, has been shown to rely on the UPR signaling pathway, although the detailed mechanisms remain poorly understood. In this study, we discovered that WSSV enhances its replication by hijacking the UPR pathway via the viral protein wsv406. Our analysis revealed a significant upregulation of wsv406 in the hemocytes and gills of infected shrimp. Mass spectrometry analysis identified that wsv406 interacts specifically with the immunoglobulin heavy-chain-binding protein (BiP) in shrimp *Litopenaeus vannamei*. Further examination revealed that wsv406 binds to multiple domains of LvBiP, inhibiting its ATPase activity without disrupting its binding to UPR stress receptors. Silencing either wsv406 or LvBiP resulted in a reduction in WSSV replication and improved shrimp survival rates. Further, wsv406 activation of the PRKR-like ER kinase (PERK)-eukaryotic translation initiation factor 2α (eIF2α) and activating transcription factor 6 (ATF6) pathways was demonstrated by a decrease in the phosphorylation of eIF2α and the nuclear translocation of ATF6 when wsv406 was silenced during WSSV infection. This activation facilitated the transcription of *WSSV* genes, promoting viral replication. In summary, these findings reveal that wsv406 manipulates the host UPR by targeting LvBiP, thereby enhancing WSSV replication through the PERK-eIF2α and ATF6 pathways. These insights into the interaction between WSSV and host cellular machinery offer potential targets for developing therapeutic interventions to control WSSV outbreaks in shrimp aquaculture.

1. Introduction

The shrimp species *Litopenaeus vannamei*, commonly known as the Pacific white shrimp, has emerged as one of the world's most commercially significant marine species (Stentiford et al., 2012) due to its adaptability to diverse environments and its rapid growth in high-density conditions. With a global aquaculture production exceeding 6.5 million tons annually, *L. vannamei* is a crucial source of high-quality animal protein worldwide. However, despite the substantial growth of shrimp farming, disease outbreaks continue to challenge the sustainability of this industry (Millard et al., 2021). Various pathogens, including viruses, bacteria, fungi, and parasites, jeopardize shrimp health (Li et al., 2019). Among these, the white spot syndrome virus (WSSV), responsible for white spot syndrome (WSS), is particularly detrimental (Siddique et al., 2018). This virus inflicts severe economic losses on the shrimp aquaculture sector, with annual losses estimated in hundreds of millions of dollars. Currently, WSS is the main pandemic in shrimp and is classified as a notifiable disease by the World Organization for Animal Health (WOAH).

WSSV, the sole member of the genus *Whispovirus*, is a bacilliform, nonoccluded, enveloped virus with a double-stranded circular DNA genome (Arulmoorthy et al., 2020). The virus has been detected in a wide range of aquatic invertebrates, predominantly among 39 families of crustaceans. Additionally, reports indicate that 13 non-crustacean

* Corresponding author.
E-mail address: lichaozh@mail2.sysu.edu.cn (C. Li).

https://doi.org/10.1016/j.virs.2024.10.005
Received 14 June 2024; Accepted 24 October 2024
Available online 28 October 2024

species can act as vectors and hosts for WSSV (Yan et al., 2004). Infection can lead to 100% cumulative mortality in shrimp within 3–10 days (Van Etten, 2009), with a replication cycle of approximately 22–24 h (Li et al., 2016). As an obligate parasite, WSSV depends entirely on the host cell's machinery for its replication and protein synthesis, folding, modification, and trafficking. The endoplasmic reticulum (ER) plays a critical role in protein folding and maturation (Walter and Ron, 2011; Wang and Kaufman, 2014). Viral replication necessitates the synthesis and folding of large quantities of proteins, which leads to the accumulation of unfolded proteins and disrupts ER homeostasis. ER stress, resulting from this accumulation of unfolded or misfolded proteins, is caused by various environmental, physiological, pathological, and nutritional factors. This stress triggers a signal-transduction cascade known as the unfolded protein response (UPR), an adaptive mechanism designed to protect cells from protein aggregates and restore ER function (Walter and Ron, 2011; Wan and Kaufman, 2014).

The UPR primarily aims to reestablish ER homeostasis by limiting mRNA translation, chaperoning misfolded proteins, and promoting cytoprotective mechanisms. It involves three parallel signaling branches: the PRKR-like ER kinase (PERK)-eukaryotic translation initiation factor 2α (eIF2α); the inositol-requiring protein 1α (IRE1α)-X-box binding protein 1 (XBP1); and the activating transcription factor 6 (ATF6) pathways. Under normal conditions, these stress receptors (PERK, IRE1, and ATF6) are inactive, bound to immunoglobulin-heavy-chain-binding protein (BiP), an ER-resident chaperone. Although the precise mechanisms of their activation under ER stress are not fully understood, it is believed that the accumulation of unfolded proteins binds preferentially to BiP, leading to its dissociation from IRE1, PERK, and ATF6. This dissociation results in the autophosphorylation of IRE1 and PERK and the mobilization of ATF6 to the Golgi apparatus for activation, subsequently triggering downstream signaling pathways. Each UPR pathway activates different target genes, collectively enabling cells to manage the stress of unfolded proteins by halting new protein synthesis and increasing their secretory capacity.

Recent research has identified key components involved in ER stress and UPR pathways in shrimp, including BiP (Luan et al., 2009), IRE1 (Chen et al., 2012), XBP1, PERK (Xu et al., 2014), eIF2α, ATF4 (Li et al., 2013), ATF6 (Yuan et al., 2017), HSP90 (Jiang et al., 2007), and calreticulin (Luana et al., 2007). Evidence suggests that UPR signaling is crucial for WSSV gene expression and proliferation. For example, LvBiP from *L. vannamei* has been cloned (Yuan et al., 2018) and implicated in UPR activation (Chen et al., 2016). RNA interference (RNAi)-mediated knockdown of LvXBP1 has been shown to reduce cumulative mortality in *L. vannamei* under WSSV infection, indicating the potential exploitation of the IRE1-XBP1 branch by WSSV (Li et al., 2013). Furthermore, silencing LvATF4 or LvATF6 results in higher survival rates, underscoring their essential roles in WSSV genome replication (Li et al., 2013; Yuan et al., 2017). These findings suggest that WSSV may hijack the UPR signaling pathway to facilitate its replication, though the precise mechanisms remain poorly understood.

In this study, we discovered that the WSSV protein wsv406 interacts with LvBiP to modulate the UPR pathway downstream of BiP, promoting WSSV replication by hijacking the PERK-eIF2α and ATF6 branches. These findings offer deeper insights into how WSSV manipulates host cellular machinery to enhance its replication, contributing to the complex understanding of the interplay between viral infection and host cellular responses.

2. Materials and methods

2.1. Shrimp and WSSV

The shrimp L. *vannamei*, each averaging 5 g, were sourced from the Hai Xingnong Company's shrimp farm in Maoming, Guangdong Province, China. These shrimp were cultured in a recirculating water tank system with aerated seawater, maintained at 27 °C and 25‰ salinity. All shrimp were specific pathogen-free (SPF) and were fed a commercial feed three times daily. Prior to the injection experiments, the shrimp underwent a three-day acclimatization period.

The WSSV, specifically the Chinese strain (GenBank accession number AF332093), was isolated from the muscle tissue of WSSV-infected shrimp and stored at −80 °C for later use (Li et al., 2018). For the experimental challenge, each shrimp was injected at the second abdominal segment with 50 μL of WSSV solution, containing approximately 1×10^5 viral copies in phosphate-buffered saline (PBS). Control shrimp received a 50 μL injection of PBS alone. Injections were administered using a 1-mL syringe.

2.2. Plasmid construction

The open reading frame (ORF) of wsv406 (GenBank accession AWQ63890.1) was cloned into pAc5.1-HA vector (Wang et al., 2021) to express HA tagged protein. The ORF of LvBiP (GenBank accession AFQ62791.1) was cloned into pAc5.1-V5 (Invitrogen, V4110-20). GFP sequence was constructed into pAc5.1-V5 to generate a GFP-pAc5.1-V5 expression vector. The different segments of LvBiP with the stop codon were cloned into GFP-pAc5.1-V5 to express N-terminal GFP-tagged recombinant proteins, respectively. For prokaryotic protein expression, wsv406 and LvBiP were cloned into pMAL-c2x (New England Biolabs, N8076S), pET-32a (+) (Merck Millipore, 69015–3) respectively. The C-terminal of coding sequences of *L. vannamei* ATF6 (GenBank accession AYM00394.1), N-terminal of coding sequences of IRE1 (GenBank accession AFQ62792.1) and PERK (GenBank accession XP_027239142.1) were cloned into pGEX-4T-1 (MiaoLing, pGEX-4T-1). The primers used were listed in Supplementary Table S1.

2.3. Co-immunoprecipitation and Western blot

To explore the potential interaction between wsv406 and BiP, LvBiP-V5 or deletion mutations of LvBiP-GFP and wsv406-HA were transfected into *Drosophila* S2 cells. After 48 h transfection, cells were harvested and washed three times using ice-cold PBS, then lysed in IP lysis buffer (Beyotime, P0013) with Protease Inhibitor Cocktail (CWBio, CW2200S) for 30 min. The supernatants were incubated with anti-V5 affinity gel beads (Sigma, A7345) at 4 °C for 2 h or anti-GFP magnetic beads (Smart-lifesciences, SM038001) at 25 °C for 1 h. The beads were washed with PBS for six times and subjected to SDS-PAGE assay as the IP sample. For input control, 10% of total cell lysate each sample was examined.

Proteins were transferred to polyvinylidene difluoride membranes. The primary antibodies used included rabbit anti-V5 antibody (Merck Millipore, AB379), rabbit anti-GFP antibody (Sigma, G1544) and rabbit anti-HA antibody (CST, 3724S). Anti-rabbit IgG HRP-conjugate (Promega, W4011) was used as the secondary antibody.

2.4. Recombinant proteins purification and pull down

The recombinant plasmids of wsv406, LvBiP, LvATF6-C, LvIRE1-N and LvPERK-N were transformed into *E. coli* Rosetta (TransGen Biotech, CD801-02) strain for expression. The MBP, His or GST tagged proteins were purified by using Amylose Resin (Smart-lifesciences, SA077025), Ni-NTA agarose (Yeasen, 20502ES50), Glutathione resin (GenScript, L00206-50) according to the manufacturer's instructions, respectively. The concentration of purified proteins was assessed with BCA kit (Fdbio science, FD2001).

For MBP pull-down assays, 100 μL (1 μg/μL) of wsv406-MBP or MBP was incubated with healthy shrimp hemocyte lysate at 4 °C for 2 h, then the Amylose Resin was added and incubated together for another 2 h at 4 °C. Next, the resin was collected and then detected using 10% SDS-PAGE and subsequent mass spectrometry analysis. Mass spectrometry was performed by Applied Protein Technology (Shanghai, China). For MBP pull-down assays, 100 μL (1 μg/μL) of wsv406-MBP was incubated with 100 μL (1 μg/μL) of LvBiP-His or Trx-His (as a control) under the same

conditions as mentioned above. Next, the resin was thoroughly washed with PBS six times. The bound proteins were eluted from resin with elution buffer (20 mM Tris-HCl pH 7.4, 0.2 M NaCl, 1 mM EDTA, 10 mM maltose) and then detected by SDS-PAGE and Western blotting. For His pull-down assays, 50 μL (1 μg/μL) of ATF6-C-GST, IRE1-N-GST or PERK-N-GST was incubated with 50 μL (1 μg/μL) of BiP and wsv406 (in a dose-dependent manner) at 4 °C for 2 h, and then the Ni-NTA resin was added and incubated for 2 h. The next steps were performed as described above except for the elution buffer (0.5 M NaCl, 20 mM Tris-HCl pH 7.4, 300 mM imidazole). The primary antibodies mouse anti-GST antibody (ABT2030), mouse anti-His antibody (ABT2050) and mouse anti-MBP antibody (ABT2070) were purchased from Abbkine.

2.5. Quantitative real-time PCR (qRT-PCR)

Total RNA extraction from different tissues and cDNA synthesis were performed as previously describe (Li et al., 2017). The expression levels of target genes were calculated using the Livak ($2^{-\Delta\Delta CT}$) relative quantification method after normalization to *L. vannamei* EF-1α (GenBank accession GU136229). Primers were listed in Supplementary Table S1.

2.6. The expression of wsv406 after WSSV challenge

For WSSV challenge experiment, the treated group was injected with 50 μL WSSV (approximately 1×10^5 copies), and the control group was injected with 50 μL PBS. Hemocytes, gills, hepatopancreas and intestines were collected at 0, 4, 12, 24, 36, 48 and 72 h post injection, and 3 samples at each time point were pooled from 9 shrimp (3 shrimp each sample). Total RNA and cDNA were prepared as illustrated above, and qRT-PCR analysis was performed as described.

2.7. Double-stranded RNA (dsRNA) synthesis

T7 RiboMAX Express RNAi System Kit (Promega, P1700) was used to generate dsRNA-wsv406, dsRNA-LvBiP and dsRNA-GFP (as a control). All Primers were listed in Supplementary Table S1.

2.8. Immunofluorescence assay

Drosophila S2 cells seeded onto poly-L-lysine-treated glass cover slips in 24-well plates at 50% confluence before transfection. 0.5 μg pAc5.1-wsv406-HA, 0.5 μg pAc5.1-LvBiP-V5 or 0.5 μg pAc5.1-wsv406-HA plus pAc5.1-LvBiP-V5 were transfected into S2 cells using the FuGENE HD Transfection Reagent (Promega, E2311), respectively. After 48 h, cells were fixed with 4% paraformaldehyde for 15 min, then they were permeabilized with methanol at −20 °C for 20 min. Next, ready-to-use goat serum (BOSTER, AR0009) was added into cells for 1 h. Then cells were incubated with a mixture of primary antibodies (rabbit anti-HA antibody, CST, 3724S; mouse anti-HA antibody, CST, 2367S; rabbit anti-V5, Abclonal, AE089; mouse anti-calnexin antibody, Proteintech, 66903–1) diluted in 2% BSA solution for 2 h. After washing slides for three times, anti-rabbit IgG (H + L), F (ab′) 2 fragment (Alexa Fluor 488 Conjugate) and anti-mouse IgG (H + L), F (ab′) 2 fragment (Alexa Fluor 594 Conjugate) were added for 1 h (1:1000 dilution). The cell nuclei were stained with Hoechst 33258 (Beyotime, C1018) and finally visualized with a confocal microscope (Leica, Stellaris 5, Germany). To explore the activation of transcription factors, shrimp were injected with dsRNA in 50 μL WSSV solution, and hemocytes were collected after 48 h. Then hemocytes were washed with PBS for three times and seeded onto slides. The following steps were the same as above, the primary antibodies used were rabbit anti-ATF4 antibody (Bioss, bs-1531R), rabbit anti-ATF6 antibody (Bioss, bs-1634R) and mouse anti-β-actin antibody (Sigma, A1978).

2.9. ATPase assays

20 μL of BiP-GST (1 μg/μL) and 40 μL of wsv406-MBP (1 μg/μL) or MBP were bounded to the GST-resin for 2 h at 4 °C, and then the resin was washed with PBS three times. 20 μM ATP was added to the resin in ATPase assay buffer (20 mM Hepes pH 7.0, 2 mM $MgCl_2$, 25 mM KCl). The remaining ATP in supernatant was measured using ATP assay kits (Beyotime, S0026) after 3 h of ATP hydrolysis reaction at 27 °C. The values were normalized using the measure of empty beads.

2.10. Phosphorylation assays

To demonstrate the phosphorylation level of LveIF2α, shrimp were injected with dsRNA-wsv406 and dsRNA-GFP (as a control) in 50 μL WSSV solution, and hemocytes and gills were collected after 48 h and lysed in lysis buffer with Phosphatase Inhibitor Cocktail (CWBio, CW2383S) and Protease Inhibitor Cocktail for 30 min. The primary antibodies used were rabbit anti-eIF2α antibody (CST, 9722S, USA), rabbit anti-*p*-eIF2α antibody (CST, 3398S, USA), rabbit anti-VP28 antibody (Genecreate, Wuhan, China) and mouse anti-β-actin antibody.

2.11. WSSV challenge experiments in shrimp treated with dswsv406 or dsLvBiP

To investigate whether wsv406 plays a positive role in WSSV challenge, healthy shrimp were separated into two groups, one injected with dsRNA-wsv406 and the other injected with dsRNA-GFP in WSSV solution. The number of surviving shrimp each group were recorded every 4 h. A parallel experiment was performed. 48 h after WSSV infection, hemocytes or gills were harvested for immunofluorescence assay, qRT-PCR and western blotting. For the quantification of WSSV copy number, nine gill tissue samples were collected. The DNA was extracted using a genomic DNA extraction kit (Genstar, D111-01), and the viral titers were measured by absolute quantitative PCR as previously describe (Xiao et al., 2020). The WSSV genome copies were calculated and normalized to 1 μg of shrimp tissue DNA.

To explore whether LvBiP participates in WSSV infection, healthy shrimp were separated into two groups and injected with dsBiP or dsGFP (2 μg/g shrimp) respectively. Then shrimp were injected with WSSV after 48 h dsRNA injection. And 48 h post WSSV infection, gills were harvested for western blotting and qRT-PCR.

2.12. XBP1 mRNA splicing assay

Shrimp were injected with dsRNA-wsv406 or dsRNA-GFP (as a control) in 50 μL WSSV solution and hemocytes and gills were collected after 48 h. The extraction of tissues RNA and reverse transcription were performed as above described. The *XBP1* gene was amplified by PCR with specific primers showed in Supplementary Table S1. Then the PCR products were digested with the restriction enzyme *Dde*I (Takara, 1248A) to distinguish the unspliced form of XBP1 (LvXBP1-u) and spliced form of XBP1 (LvXBP1-s) and separated using 1.5% agarose gel.

2.13. Statistical analysis

All data were presented as mean ± SD. Student's *t*-test was used to calculate the comparisons among groups of numerical data. The following *P*-values were considered statistically significant: $^{**}P < 0.01$, $^{*}P < 0.05$. For survival rates, data were subjected to statistical analysis using GraphPad Prism software to generate the Kaplan-Meier plots (log-rank $\chi 2$ test).

3. Results

3.1. Expression of wsv406 in WSSV-challenged shrimp

To elucidate the expression profiles of wsv406, we performed quantitative RT-PCR to analyze its time-course expression following WSSV challenge. Hemocytes, gills, hepatopancreas, and intestines, which are crucial immune organs involved in the defense against pathogens in shrimp (Tassanakajon et al., 2011), were examined for wsv406 expression. In hemocytes, wsv406 expression was rapidly upregulated, showing a ~1.78-fold increase at 12 h post-infection. The expression remained elevated from 36 to 72 h, with significant increases of ~4.54-, ~59.23-, and ~126.52-fold, respectively (Fig. 1A). In the gills of WSSV-infected shrimp, wsv406 expression was markedly upregulated during the late stages of infection, exhibiting ~33.28-, ~84.21-, and ~64.01-fold increases at 36, 48, and 72 h, respectively (Fig. 1B). In the hepatopancreas, a slight upregulation of wsv406 was observed at 36 h post-infection (Fig. 1C). The intestines showed significant upregulation of wsv406 at 24 h (~1.44-fold), 36 h (~3.68-fold), 48 h (~2.18-fold), and 72 h (~3.11-fold) post-infection (Fig. 1D). These results suggest that wsv406 is primarily expressed during the late stages (36–72 h) of WSSV infection in hemocytes and gills. Therefore, we selected hemocytes and gills as the main tissues for subsequent experiments.

3.2. Identification of the wsv406-interacting protein in shrimp

To identify the protein that interacts with wsv406, we purified wsv406-MBP (maltose-binding protein) and MBP (as a control) and incubated them with shrimp hemocyte lysate. The captured proteins were separated by SDS-PAGE and identified using LC-MS/MS (Fig. 2A). The analysis revealed several candidate proteins, including hemocyanin, prophenoloxidase 2, heat shock protein 70 (HSP70), BiP, and ATP synthase subunit alpha (Fig. 2B). Proteins matching two or more unique peptides were classified as high-confidence interactors. Among these, BiP stood out as a high-confidence interactor with multiple peptide matches (Fig. 2C and D). Notably, hemocyanin (Wang et al., 2022), prophenoloxidase 2 (Ai et al., 2009) and HSP70 (Janewanthanakul et al., 2020) are well-documented for their roles during WSSV infection. However, BiP, a molecular chaperone, had not been previously characterized for its function in the context of WSSV infection, emerged as a particularly intriguing candidate. Therefore, LvBiP was selected for more detailed study.

3.3. Interaction of wsv406 with multiple regions of LvBiP

To explore the specificity of the interaction between wsv406 and LvBiP, we conducted a pull-down assay. We expressed and purified MBP-tagged wsv406, His-tagged LvBiP, and Trx-His. The MBP-tag pull-down assay revealed that wsv406 precipitated LvBiP, a result confirmed by Western blotting with an anti-His antibody (Fig. 3A). Since shrimp cell lines are unavailable, we used Co-immunoprecipitation (Co-IP) assays in *Drosophila* S2 cells to confirm that wsv406 interacts with LvBiP (Fig. 3B). Previous studies have established that BiP is an ER protein, which we corroborated through immunofluorescence experiments showing that BiP co-localizes with the ER marker protein calnexin (Paskevicius et al., 2023) (Fig. 3C). Similarly, wsv406 was found to co-localize with both calnexin and BiP, confirming their interaction.

BiP, a highly conserved chaperone of the heat shock protein 70 (HSP70) family, contains an ATPase domain (124–278 aa) at the N-terminal and a peptide-binding domain (398–498 aa) at the C-terminal (Yuan et al., 2018). To determine which domain of BiP mediates its interaction with wsv406, we generated several truncated mutants of LvBiP (Fig. 3D): LvBiP-AD (only the ATPase domain), LvBiP-PBD (only the peptide-binding domain), LvBiP-mAD (missing the ATPase domain), LvBiP-mPBD (missing the peptide-binding domain), LvBiP-AP (only the linker between the ATPase and peptide-binding domains), and LvBiP-mAP (missing the linker). Co-IP assays indicated that all truncated mutants could associate with wsv406, suggesting that the ATPase domain, peptide-binding domain, and linker of LvBiP can interact with wsv406 (Fig. 3E).

3.4. Inhibition of LvBiP's ATPase activity by wsv406

The UPR is a cellular adaptive mechanism activated in response to the accumulation of unfolded or misfolded proteins in the ER. Under non-stress conditions, the chaperone protein BiP binds to and maintains the ER stress receptors PERK, IRE1, and ATF6 in an inactive state. During ER stress, BiP dissociates from these receptors, triggering their activation (Bertolotti et al., 2000; Shen et al., 2002; Walter and Ron, 2011). To investigate whether the interaction of wsv406 with BiP influences BiP's binding to these stress receptors, we conducted competitive pull-down assays. For this purpose, we purified His-tagged LvBiP and GST-tagged ER lumen domains of LvATF6 (ATF6-C-GST), LvIRE1 (IRE1-N-GST), and LvPERK (PERK-N-GST) (Supplementary Fig. S1). We then incubated these proteins with increasing concentrations of MBP-tagged wsv406.

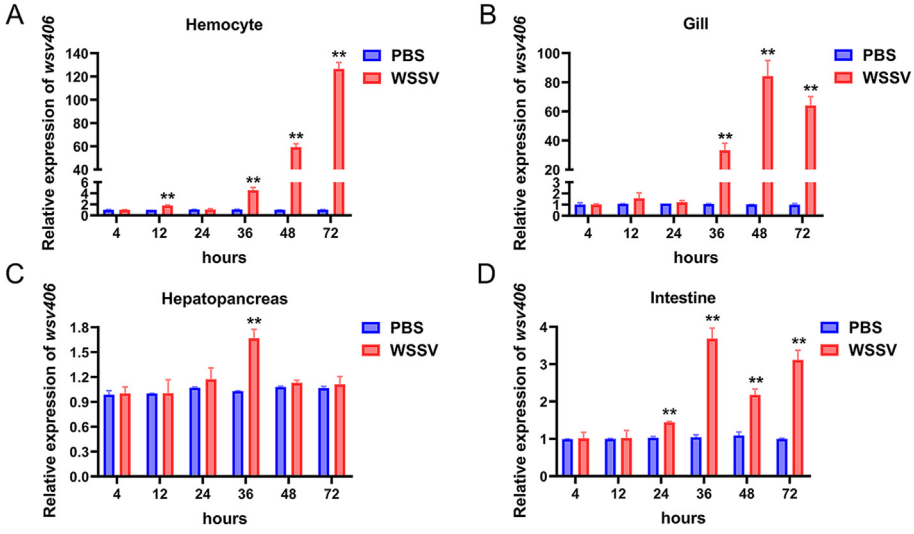

Fig. 1. Expression of wsv406 in WSSV-challenged shrimp. Expression profiles of wsv406 after WSSV infection in hemocytes (**A**), gills (**B**), hepatopancreas (**C**), intestine (**D**) were detected by qRT-PCR. All experiments were performed three times. All the data were analyzed by Student's *t*-test (*$P < 0.05$, **$P < 0.01$).

A

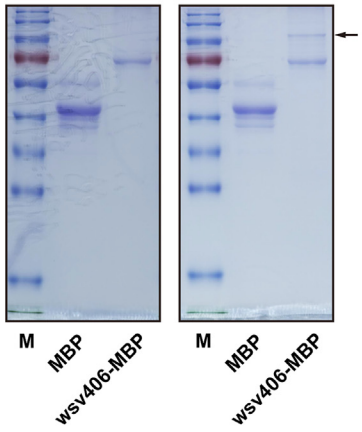

B

Selected candidates for wsv406-binding proteins from the LC-MS/MS identified proteins

Uniprot ID	Protein Name	Unique PepCount	Cover Percent	PI
A0A3R7Q123	Hemocyanin	26	34.42%	5.31
A5JSX2	Prophenoloxidase 2	8	8.25%	6.05
A0A423SC79	Heat shock protein 70	6	11.88%	5.34
J7K1E9	BiP	3	5.50%	4.98
D3W7E4	ATP synthase subunit alpha	3	4.73%	8.97

C

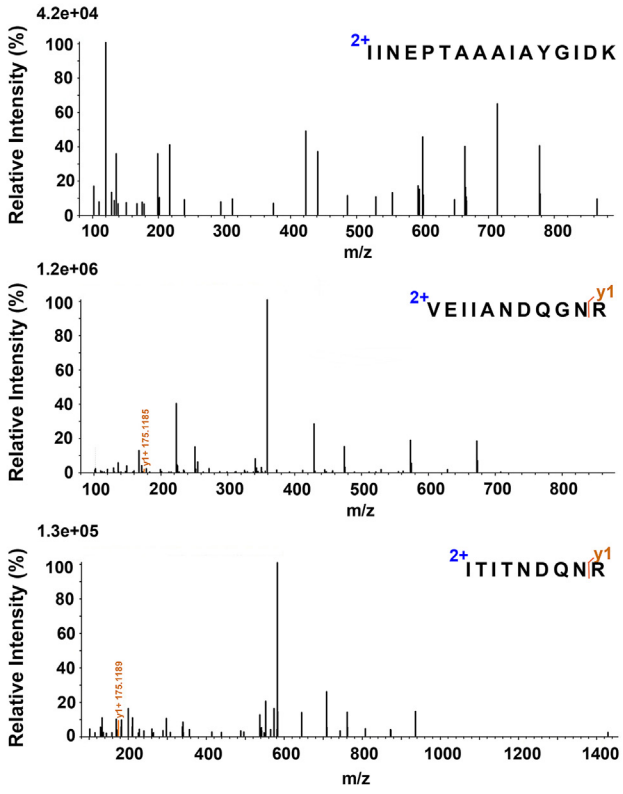

D

>ROT68763.1 Bip [*Litopenaeus vannamei*]

MRCWTALAAIAAVMAVAATAKDKKEEVGTVIGIDLGTTYSCVGVF

KNG**RVEIIANDQGNRI**TPSYVAFTADGERLIGDSAKNQLTTNPEN

TVFDAKRLIGREWTDKSVQHDIQFFPFKVINKNDKPHIKVSTTQG

EKVFAAEEISAMVLGKMKETAEAYLGKTVTHAVVTVPAYFNDAQR

QATKDAGTIAGLTVM**RIINEPTAAAIAYGIDKK**DGEKNILVFDLGG

GTFDVSLLTIDSGVFEVVATNGDTHLGGEDFDQRVMDHFIKLYKK

KKGKDIRKDNRAVQKLRREVEKAKRSLSSSHQVRIEIESFFEGDD

FSETLTRAKFEELNMDLFRSTMKPVQKVLEDSDLQKKEIDEIVLV

GGSTRIPKIQQLVKEFFGGKEPSRGINPDEAVAYGAAVQAGVLSG

EDDTNDLVLLDVNPLTLGIETVGGVMTKLIPRNTVIPTKKSQIFSTA

SDNQHTVTIQVFEGERPMTKDNHILGKFDLTGIPPAPRGVPQIEV

TFEIDANGILQVSAEDKGTGNKE**KITITNDQNRL**TPEDIERMIKDA

EVFADEDKKLKERVESRNELESYAYSLKNQINDKEKLGAKLSDED

KEKMEEAIEEKIKWLEDNPESDAEDYKTQKKELEDVVQPIITKLYQ

QSGEAPPPTEDGEDYEKDEL

Fig. 2. Identification of wsv406 binding proteins by pull-down experiments and mass spectrometry. **A** Recombination expression and purification of MBP, MBP-tagged wsv406. MBP-pulldown assay to detect the interaction with wsv406 in hemocytes. Potentially interacting proteins were represented by black arrow. **B** Selected candidates for wsv406-binding proteins from the LC-MS/MS identified proteins. **C** The secondary mass spectrometry of the target peptides of LvBiP. **D** Location of the target peptide identified by mass spectrometry on the BiP.

The results indicated that higher doses of wsv406 increased its precipitation with BiP, while BiP's interactions with ATF6, IRE1, and PERK remained unaffected (Fig. 4A).

Given that BiP's ATPase activity is crucial for its function as a chaperone involved in protein folding, assembly, trafficking, and quality control (Gething, 1999), we investigated whether wsv406 influences this activity. We incubated BiP-GST with either wsv406-MBP or MBP (as a control) in an ATPase assay buffer and measured ATP hydrolysis efficiency (Fig. 4B). The values were normalized using the measure of empty beads. BiP incubated with wsv406 exhibited significantly reduced ATPase activity compared to BiP incubated with MBP (Fig. 4C). These findings indicate that wsv406 does not interfere with LvBiP's interaction with ATF6, IRE1, and PERK but does inhibit BiP's ATPase activity.

3.5. *wsv406 and LvBiP facilitate WSSV replication in shrimp*

Given that wsv406 interacts with LvBiP and affects its function (ATPase activity), we hypothesized that both wsv406 and LvBiP may positively influence WSSV replication. To test this, we silenced the expression of wsv406 in WSSV-infected shrimp using RNAi (Fig. 5A). Quantitative RT-PCR confirmed a significant reduction in wsv406 mRNA levels (~0.27-fold) in the gills at 48 h post-WSSV infection in the dsRNA-wsv406 group compared to the dsRNA-GFP control group (Fig. 5B). Following WSSV or PBS (mock) challenge, we recorded shrimp mortality every 4 h. The survival rate was significantly higher in the dsRNA-wsv406 group compared to the control ($P = 0.0078$) (Fig. 5C). No deaths were observed in shrimp injected with dsRNA and PBS, indicating that dsRNA injection itself did not cause mortality (Fig. 5C). We further

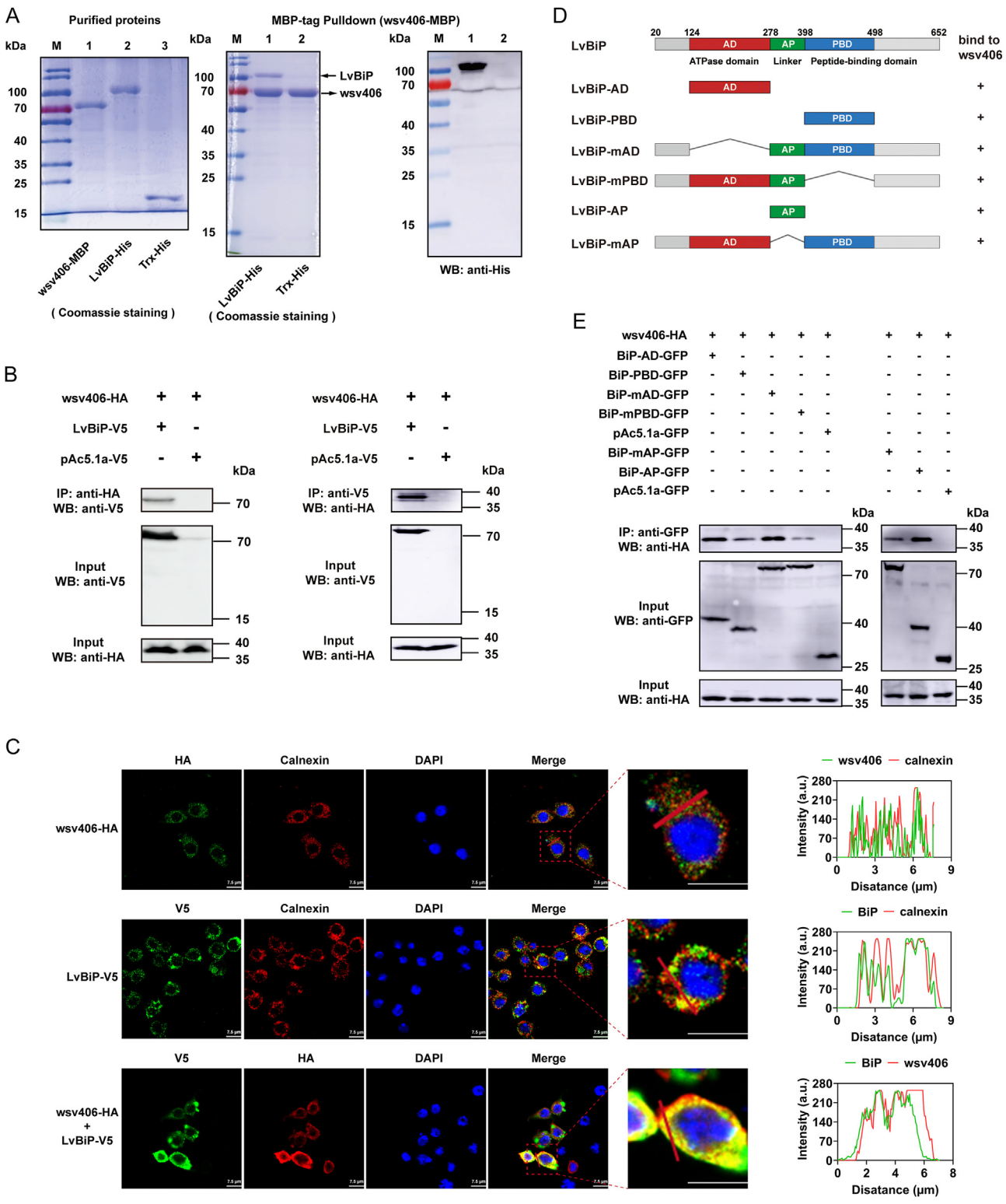

Fig. 3. Wsv406 interacts with LvBiP. **A** Purified MBP-tagged wsv406, His-tagged BiP and Trx-His. wsv406 interacted with BiP was confirmed in MBP-pulldown, as shown by staining with Coomassie blue and western blotting. **B** Co-IP assays showed wsv406 interacted with BiP. **C** Subcellular localization of wsv406, BiP and colocalization of 406 with BiP in *Drosophila* S2 cells. Colocalization was analyzed by Image J. Calnexin, ER indicator. Scale bar, 7.5 μm. **D** Schematic diagram of LvBiP deletion mutation constructs. **E** The Co-IP assays confirmed the interaction between wsv406 and the mutations of BiP.

quantified viral loads in the gills using absolute qPCR. The WSSV genomic copies in the dsRNA-wsv406 + WSSV group were lower than in the dsRNA-GFP + WSSV group (Fig. 5D). Similarly, the transcript and protein levels of VP28 were significantly reduced in the dsRNA-wsv406 + WSSV group compared to controls (Fig. 5E).

To explore the role of BiP in WSSV replication, we injected shrimp with dsRNA targeting LvBiP (dsBiP) followed by WSSV infection (Fig. 5F). Knockdown of LvBiP led to a significant reduction in BiP transcription (~0.26-fold) compared to the dsGFP group (Fig. 5G). Analysis of viral copies (Fig. 5H) and VP28 levels (Fig. 5I) showed that

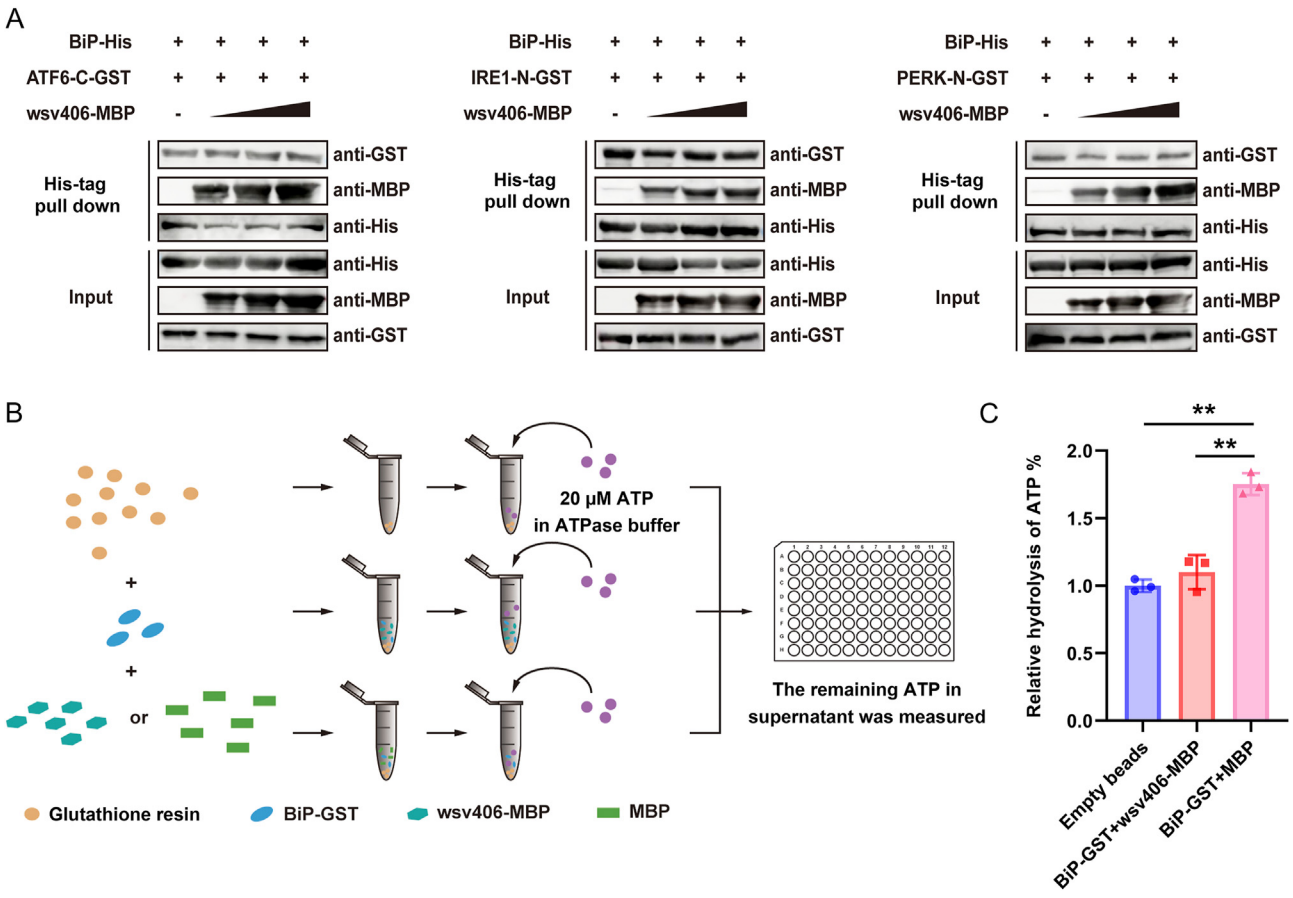

Fig. 4. Wsv406 doesn't interfere the interaction of LvBiP with ATF6, IRE1 and PERK, but suppresses LvBiP ATPase activity. **A** His-tag pulldown for the detection of the interaction between BiP and ATF6, IRE1 or PERK by expression of wsv406 in a dose-dependent manner. The results were shown via western blotting. **B** Schematic representation of the procedures for measuring the ATPase activity of BiP. **C** ATPase activity of the recombinant BiP. GST-BiP were bound to Glutathione beads and MBP-wsv406 or MBP and then assessed for the ATPase activity. The values were normalized using the measure of empty beads.

silencing LvBiP reduced WSSV replication. Collectively, these results suggest that both wsv406 and LvBiP are essential for WSSV replication.

3.6. *wsv406 regulates the UPR pathway during WSSV infection*

To investigate how wsv406 affects the UPR pathway downstream of LvBiP, we analyzed indicators of the three UPR pathways. Under ER stress, the PERK-eIF2α pathway is activated. PERK phosphorylates eIF2α, which reduces the frequency of AUG initiation codon recognition, thereby inhibiting global mRNA translation while selectively enhancing the translation of mRNAs like ATF4. ATF4 then translocates to the nucleus to trigger the expression of various genes (Wang and Kaufman, 2014). We first assessed the phosphorylation level of eIF2α. Knockdown of wsv406 significantly reduced eIF2α phosphorylation in hemocytes and gills compared to the dsGFP-treated group (Fig. 6A; Supplementary Fig. S2), indicating that wsv406 silencing suppresses the activation of the PERK-eIF2α pathway. Immunofluorescence assays confirmed reduced nuclear import of ATF4 in hemocytes from the dsRNA-wsv406 group compared to the dsGFP group (Fig. 6B). Consistent with these findings, qRT-PCR showed decreased expression of ATF4-regulated viral genes (*wsv023, wsv069, wsv064, wsv256, wsv303, wsv343*) in hemocytes and gills from the dsRNA-wsv406 group compared to controls (Fig. 6C).

Activation of the ATF6 pathway involves ATF6 dissociating from BiP and translocating to the Golgi apparatus, where it is cleaved by site 1 protease (S1P) and site 2 protease (S2P), producing the active transcription factor ATF6s. ATF6s then enters the nucleus and initiates the transcription of target genes (Wang and Kaufman, 2014). We examined whether wsv406 affects this pathway by assessing the nuclear translocation of LvATF6 and the expression of LvATF6-regulated genes. Compared to the control group (dsGFP + WSSV), the nuclear translocation of LvATF6 was reduced in the wsv406-knockdown group (Fig. 7A). Interestingly, wsv406 knockdown upregulated the expression of apoptosis signal-regulating kinase 1 (LvASK1) in the hemocytes of WSSV-infected shrimp (Fig. 7B), consistent with previous reports that ATF6 activation downregulates LvASK1 expression (Yuan et al., 2017). Additionally, qRT-PCR showed that knockdown of wsv406 downregulated the expression of LvXBP1 (Fig. 7C) and LvATF6-regulated viral genes (*wsv023, wsv045, wsv083, wsv222, wsv249, wsv343*) (Fig. 7D). These findings suggest that silencing wsv406 inhibits the activation of the ATF6 pathway.

Under non-stress conditions, IRE1 is inactive due to its interaction with BiP. Upon release from BiP, IRE1 activates its kinase and endoribonuclease (RNase) activities, leading to the splicing of XBP1 mRNA. Similar to mammalian and *Drosophila* XBP1 mRNA, LvXBP1 mRNA contains splicing motifs that can be targeted by the endonuclease *Dde*I. We identified the sequence "CAGTATCCCAACCTCAG" in LvXBP1, which includes the *Dde*I restriction site (CTNAG) (Supplementary Fig. S3A). Using primers designed for LvXBP1 (Supplementary Table S1), we performed PCR, followed by *Dde*I digestion. Unspliced XBP1 (LvXBP1-u) is cleaved by *Dde*I, producing a shorter fragment, while spliced XBP1 (LvXBP1-s) remains intact. Supplementary Fig. S3B shows that WSSV infection increased XBP1-s levels (lanes 2–3) compared to uninfected controls (lane 1), consistent with the activation of the IRE1 pathway by WSSV infection (Chen et al., 2012). However, knockdown of wsv406 did not significantly alter XBP1-s levels, suggesting that silencing wsv406 does not impact the IRE1-XBP1 pathway.

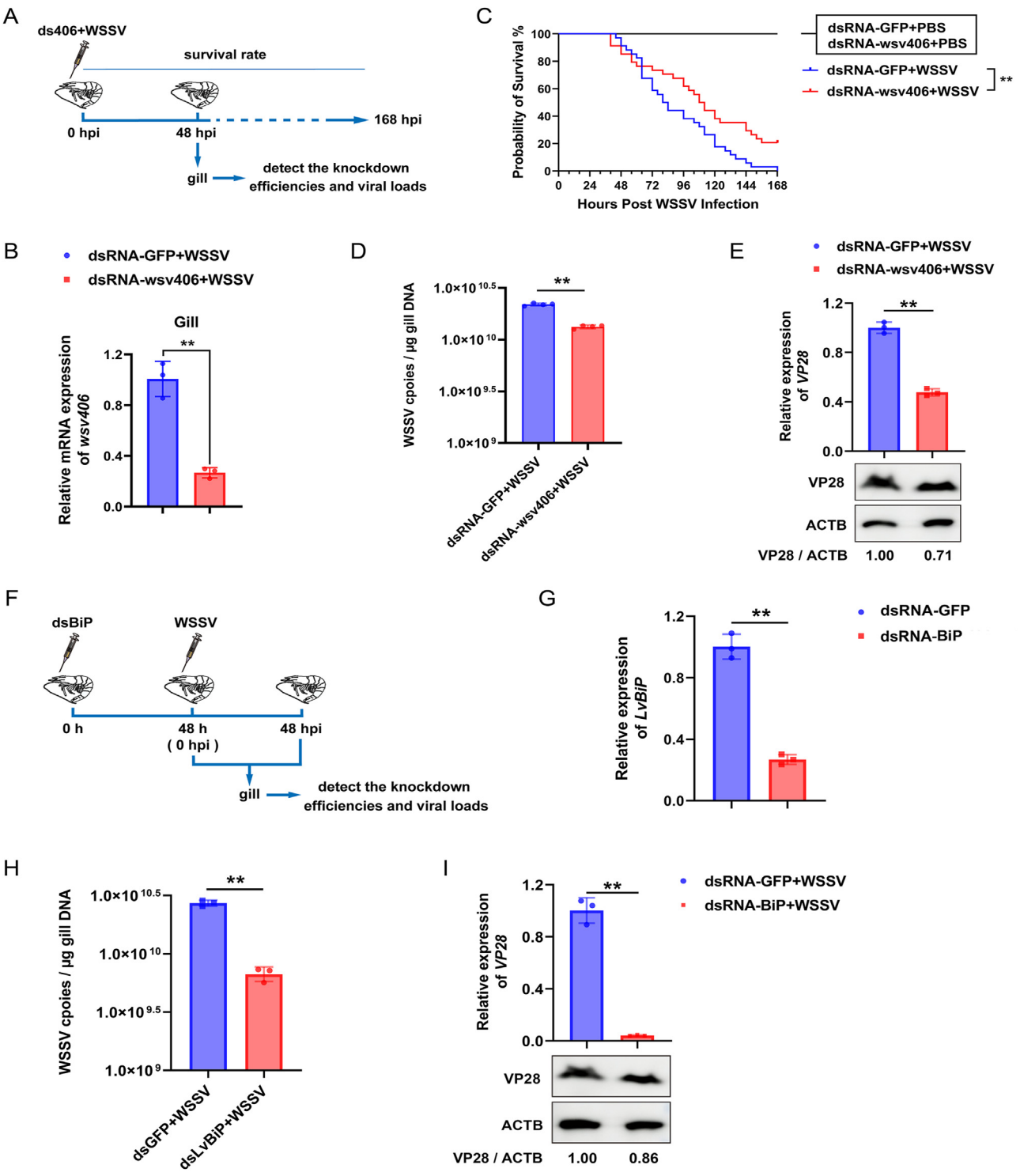

Fig. 5. Wsv406 and BiP are crucial for WSSV replication and pathogenicity. **A** Schematic illustration of the experimental procedure for exploring the effect of wsv406 on WSSV pathogenicity. **B** The silencing efficiencies of wsv406 at 48 h after injection with dsRNA and WSSV. The gills from nine shrimp were sampled and pooled. **C** Survival of wsv406-silenced shrimp with WSSV challenge. Differences in cumulative mortality levels between groups were analyzed by log-rank (Mantel-Cox) test (**$P < 0.01$). **D** The copies of WSSV in gills of dswsv406 or dsGFP treated shrimp at 48 h after WSSV infection. **E** The expression level of VP28 in gills. The mRNA levels and protein levels were detected by quantitative RT-PCR (upper panel) and western blotting (lower panel) at 48 h after WSSV injection, respectively. Beta actin was used as a protein loading control, and the relative grayscale values of VP28/actin were showed. **F** Schematic diagram of procedure for investigating the influence of BiP on WSSV replication. **G** Knockdown efficiency of BiP was checked by qRT-PCR at 48 h post dsRNA infection. **H** Silencing of BiP reduced WSSV replication in gills at 48 hpi via absolute quantitative PCR assay. **I** The gills were checked by qRT-PCR (mRNA levels) and western blotting (protein levels) for the expression level of VP28. Beta actin was used as a protein loading control, and the relative grayscale values of VP28/actin were showed. The data (**B**, **D**, **E**, **G**–**I**) were analyzed statistically by Student's *t*-test (*$P < 0.05$, **$P < 0.01$).

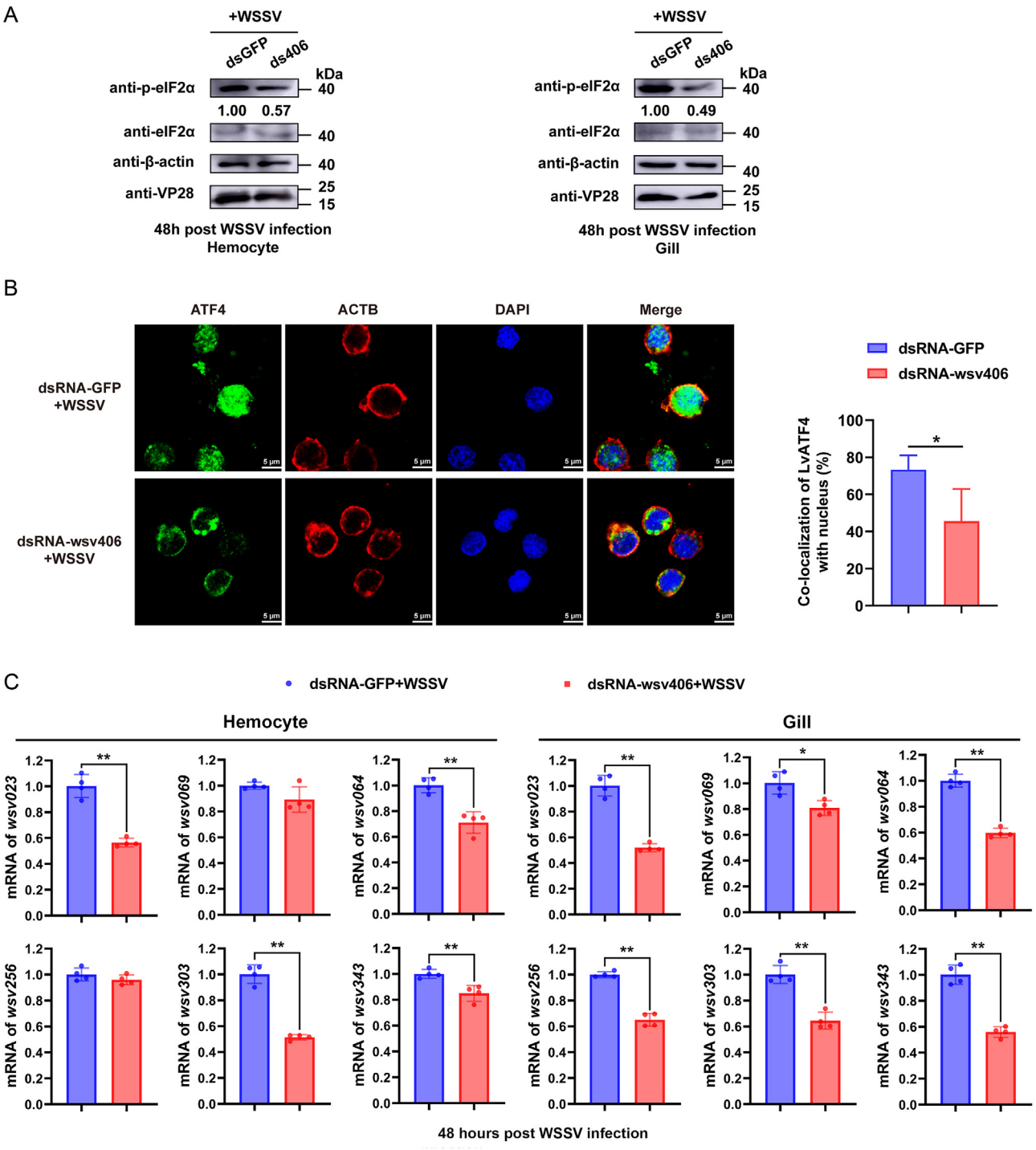

Fig. 6. Knockdown of wsv406 downregulates PERK-eIF2α pathway during WSSV infection *in vivo*. **A** The phosphorylation of eIF2α was detected in hemocyte (left panel) and gill (right panel) at 48 h post WSSV infection by western blotting. Beta-actin was used as a loading control to calculate the ratio of *p*-eIF2α/eIF2α. VP28 served as the indicator for infection. **B** LvATF4 nuclear translocation was inhibited in wsv406-silenced hemocytes. The Image J software calculated the percentage of ATF4 into the nucleus. **C** Viral genes expression levels in hemocyte (left panel) and gill (right panel) of dswsv406-treated shrimp at 48 h post WSSV infection were detected by qRT-PCR. The data were provided as the means ± SD of triplicate assays and analyzed statistically by Student's *t*-test (**$P < 0.01$).

4. Discussion

Viruses rely entirely on host cells to complete their life cycle, encompassing gene replication, protein synthesis, and the production of new virions. Viral infections induce ER stress as the replication process demands the synthesis and folding of numerous proteins, leading to their accumulation in the ER lumen. This stress activates the UPR signaling pathways. A substantial body of research highlights that pathogens co-evolve with their hosts and develop sophisticated strategies to evade and exploit host immune defenses. The UPR is critical for maintaining ER homeostasis, and it is well-documented that viruses often hijack these pathways to benefit their replication. For instance, the Dengue virus (DENV) sequentially activates different UPR pathways at distinct stages of infection to sustain its lifecycle: the PERK-eIF2α branch during early infection (Umareddy et al., 2007; Peña and Harris, 2011), the IRE1-XBP1 branch during the middle stages (Yu et al., 2006), and the ATF6 branch

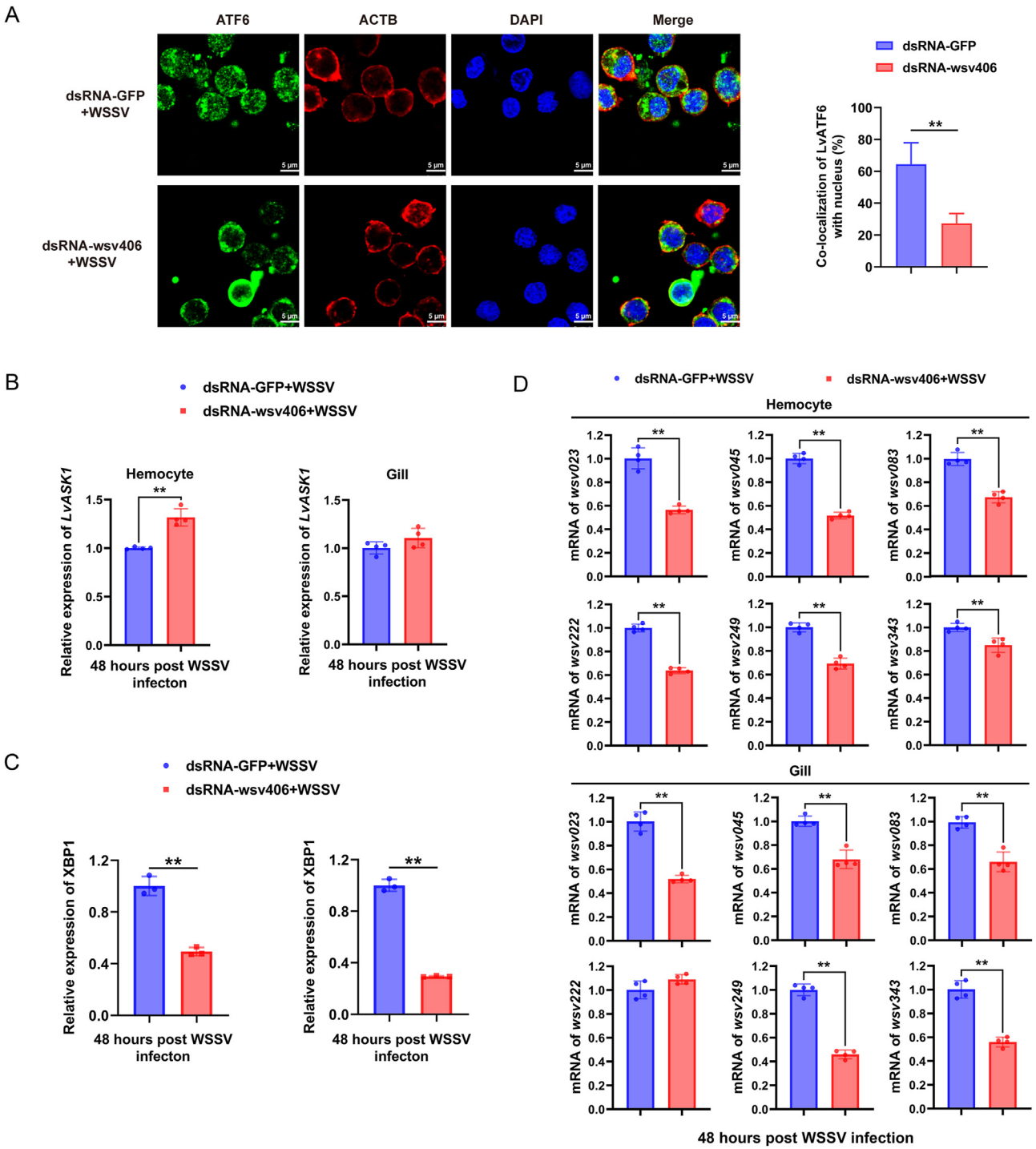

Fig. 7. Effects of wsv406 knockdown on ATF6 pathway during WSSV infection. **A** Transcription factor LvATF6 nuclear translocation in wsv406 silenced hemocytes infected by WSSV. The percentage of ATF6 nuclear translocation was calculated by Image J. The scale bar = 5 μm. **B–D** Expression levels of LvASK1 (**B**), LvXBP1 (**C**) and WSSV genes (**D**) in hemocytes and gills of dsRNA-GFP treated or dsRNA-wsv406 treated shrimps at 48 h post WSSV infection. Differences were analyzed using Student's *t*-test (**$P < 0.01$).

during late infection (Peña and Harris, 2011). Similarly, Human Cytomegalovirus (HCMV) manipulates the UPR to facilitate its replication, notably without the typical translation inhibition usually caused by phosphorylated eIF2α (Isler et al., 2005). The African swine fever virus (ASFV) also modulates the UPR by activating the ATF6 pathway, upregulating the chaperone calreticulin, and inhibiting the C/EBP homologous protein (CHOP) apoptosis pathway to promote replication (Galindo et al., 2012). These examples illustrate that a variety of viruses can induce or hijack the UPR to their advantage. However, there is limited knowledge about the specific mechanism viruses employ to manipulate UPR signaling pathways. Our study provides new insights by demonstrating that WSSV exploits the host's PERK-eIF2α and ATF6 branches of the UPR to enhance its replication by targeting the molecular chaperone LvBiP (Fig. 8).

BiP, also known as glucose-regulated protein 78 (GRP78), is a key chaperone protein of the HSP70 family. BiP's crucial role in viral infection and replication is evidenced by its interactions with various viruses. For instance, during the COVID-19 pandemic caused by SARS-CoV-2,

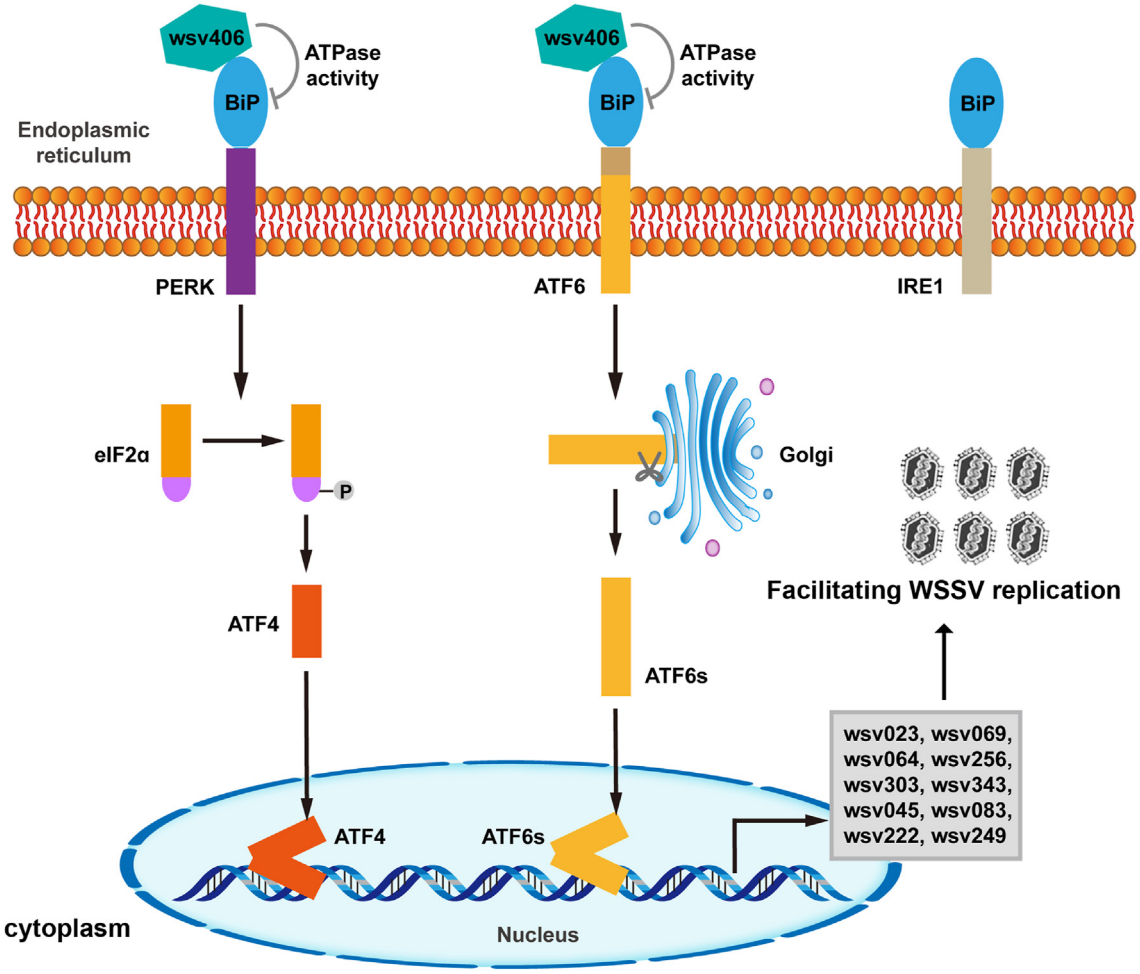

Fig. 8. The possible model illustrating that WSSV hijacks UPR signaling through wsv406 targeting BiP that facilitates to WSSV replication. In WSSV-infected shrimp, the viral protein wsv406 interacts with and inhibits the ATPase activity of the host protein BiP. This interaction leads to the activation of the PERK-eIF2α and ATF6 pathways, which subsequently promote the expression of other viral genes, facilitating WSSV replication.

elevated BiP levels were found in several host proteins associated with viral invasion, underscoring BiP's importance in facilitating viral entry and infection (Elfiky, 2020; Ibrahim et al., 2020). BiP has been identified as a pro-viral protein in SARS-CoV-2 infections (Shin et al., 2022). Moreover, BiP interacts with the E protein of dengue virus serotype 2 (DENV2) in the mosquito cell line *Aedes albopictus* C6/36, and silencing BiP reduces viral E protein levels (Chen et al., 2017). In our study, LvBiP was identified as a protein interacting with wsv406 through mass spectrometry, and this interaction was further validated using pull-down assays, Co-IP and immunofluorescence. Normally, BiP binds to the UPR stress receptors PERK, IRE1, and ATF6, keeping them in an inactive state. However, our results indicated that increasing the dose of wsv406 did not disrupt LvBiP's binding to UPR stress receptors. Notably, viral proteins often interact with proteins possessing ATPase activity, influencing their function (Jiang et al., 2020). We assessed the ATPase activity of LvBiP in the presence of wsv406 and found that wsv406 inhibited LvBiP's ATPase activity. We thus hypothesize that wsv406 inhibits LvBiP's ATPase activity, thereby inducing ER stress and triggering the UPR to facilitate its own replication. Supporting this hypothesis, RNAi knockdown of wsv406 or LvBiP resulted in reduced viral copies and lower VP28 levels in WSSV-infected shrimp.

In the context of UPR signaling, transcription factors such as XBP1, ATF4, and ATF6 serve as critical intermediaries, linking upstream unfolded protein signals to downstream gene regulation (Schröder and Kaufman, 2005). These transcription factors bind to specific elements in target gene promoters, like ESRE-I, ESRE-II, and ATF/CREN AP1, to regulate gene transcription. Previous studies have shown that *L. vannamei* ATF4 can regulate the promoter activity of several WSSV genes (*wsv023, wsv064, wsv069, wsv256, wsv303, wsv343*) *in vitro* (Li et al., 2013). Similarly, ATF6 can regulate the expression of other viral genes, including *wsv023, wsv045, wsv083, wsv129, wsv222, wsv249,* and *wsv343* (Yuan et al., 2017). Another shrimp transcription factor, ATFβ, induces the expression of viral genes *wsv059* and *wsv166* in insect cells (Li et al., 2014). In the PERK-eIF2α pathway, the phosphorylation of eIF2α typically inhibits global protein translation. However, some viruses have evolved mechanisms to bypass this inhibition. For example, HCMV infection increases eIF2α phosphorylation but does not significantly impede overall protein translation (Isler et al., 2005). Our findings indicate that wsv406 activates the PERK-eIF2α pathway and elevates eIF2α phosphorylation levels. While it remains to be verified if this affects overall translation, wsv406 also upregulated the transcription of several viral genes (*wsv023, wsv069, wsv064, wsv256, wsv303, wsv343*) through ATF4, aligning with prior observations that ATF4 knockdown reduces WSSV-induced mortality in shrimp (Li et al., 2013). In the ATF6 branch of the UPR, wsv406 knockdown significantly inhibited ATF6 signaling, as evidenced by reduced transcription of ATF6-regulated viral genes (*wsv023, wsv045, wsv083, wsv222, wsv249, wsv343*). Interestingly, ASK1 transcription was upregulated in hemocytes of WSSV-infected shrimp following wsv406 knockdown. Previous research indicates that silencing ATF6 increases apoptosis and that LvATF6 reduces apoptosis in actinomycin-treated *Drosophila* S2 cells, suggesting LvATF6 has anti-apoptotic properties (Yuan et al., 2017). Our data suggest that wsv406 may activate ATF6 to downregulate ASK1, thereby negatively regulating

the ASK1-JNK-*c*-Jun pathway and reducing apoptosis, thus promoting viral replication. The observation that ASK1 transcription levels were not significantly different in the gills of the wsv406-knockdown group compared to controls might be due to the higher expression of ASK1 in hemocytes, where apoptosis predominantly occurs (Yuan et al., 2016). Furthermore, the viral protein wsv222, which acts as an E3 ubiquitin ligase in the ubiquitination pathway, mediates the degradation of tumor suppressor-like protein (TSL) and plays an anti-apoptotic role in WSSV-infected shrimp (He et al., 2006). Activation of ATF6 by wsv406 to upregulate wsv222 transcription likely reduces cell apoptosis, aiding viral replication. Surprisingly, we found that wsv406 did not significantly affect the IRE1-XBP1 pathway, as assessed by XBP1 splicing. However, the exact mechanisms by which wsv406 interacts with and influences the IRE1-XBP1 pathway require further investigation.

5. Conclusions

In summary, our study demonstrates that WSSV manipulates the host's PERK-eIF2α and ATF6 pathways via the viral protein wsv406 via targeting the chaperone protein BiP, which facilitates viral gene expression and replication. These findings enhance our understanding of the molecular mechanisms through which WSSV exploits the UPR to promote its life cycle, and provide a foundation for developing innovative strategies to prevent and control WSSV infections, potentially leading to more effective interventions in shrimp aquaculture.

Ethics statement

All animal experiments were approved by Institutional Animal Care and Use Committee of Sun Yat-Sen University (Approval No. SYSU-IACUC-2023-B0005).

Author contributions

Shihan Chen: conceptualization, investigation, formal analysis, writing – original draft. Qiqi Zhong: investigation, formal analysis. Xuzheng Liao: investigation. Haiyang Wang: investigation. Bang Xiao: investigation. Jianguo He: conceptualization, formal analysis, project administration, resources. Chaozheng Li: conceptualization, formal analysis, funding acquisition, project administration, resources, writing – original draft, writing – review editing.

Data availability

All the data generated during the current study are included in the manuscript.

Conflict of interest

All authors declare that there are no competing interests.

Acknowledgements

This research was supported by the Southern Marine Science and Engineering Guangdong Laboratory (Zhuhai) (SML2023SP234), National Natural Science Foundation of China (32022085/32373158/31930113), and the open competition program of top ten critical priorities of Agricultural Science and Technology Innovation for the 14th Five-Year Plan of Guangdong Province (2022SDZG01). The funders had no role in study design, data collection and analysis, decision to publish, or preparation of the manuscript.

Appendix A. Supplementary data

Supplementary data to this article can be found online at https://doi.org/10.1016/j.virs.2024.10.005.

References

Ai, H.S., Liao, J.X., Huang, X.D., Yin, Z.X., Weng, S.P., Zhao, Z.Y., Li, S.D., Yu, X.Q., He, J.G., 2009. A novel prophenoloxidase 2 exists in shrimp hemocytes. Dev. Comp. Immunol. 33, 59–68.

Arulmoorthy, M.P., Anandajothi, E., Vasudevan, S., Suresh, E., 2020. Major viral diseases in culturable penaeid shrimps: a review. Aquacult. Int. 28, 1939–1967.

Bertolotti, A., Zhang, Y.H., Hendershot, L.M., Harding, H.P., Ron, D., 2000. Dynamic interaction of BiP and ER stress transducers in the unfolded-protein response. Nat. Cell Biol. 2, 326–332.

Chen, Y.H., Zhao, L., Pang, L.R., Li, X.Y., Weng, S.P., He, J.G., 2012. Identification and characterization of Inositol-requiring enzyme-1 and X-box binding protein 1, two proteins involved in the unfolded protein response of *Litopenaeus vannamei*. Dev. Comp. Immunol. 38, 66–77.

Chen, Y.H., Yuan, F.H., Bi, H.T., Zhang, Z.Z., Yue, H.T., Yuan, K., Chen, Y.G., Weng, S.P., He, J.G., 2016. Transcriptome analysis of the unfolded protein response in hemocytes of *Litopenaeus vannamei*. Fish Shellfish Immunol. 54, 153–163.

Chen, T.H., Chiang, Y.H., Hou, J.N., Cheng, C.C., Sofiyatun, E., Chiu, C.H., Chen, W.J., 2017. XBP1-mediated BiP/GRP78 upregulation copes with oxidative stress in mosquito cells during dengue 2 virus infection. BioMed Res. Int. 2017, 3519158.

Elfiky, A.A., 2020. SARS-CoV-2 spike-heat shock protein A5 (GRP78) recognition may be related to the immersed human coronaviruses. Front. Pharmacol. 11, 577467.

Galindo, I., Hernáez, B., Muñoz-Moreno, R., Cuesta-Geijo, M.A., Dalmau-Mena, I., Alonso, C., 2012. The ATF6 branch of unfolded protein response and apoptosis are activated to promote African swine fever virus infection. Cell Death Dis. 3, e341.

Gething, M.J., 1999. Role and regulation of the ER chaperone BiP. Semin. Cell Dev. Biol. 10, 465–472.

He, F., Fenner, B.J., Godwin, A.K., Kwang, J., 2006. White spot syndrome virus open reading frame 222 encodes a viral E3 ligase and mediates degradation of a host tumor suppressor via ubiquitination. J. Virol. 80, 3884–3892.

Ibrahim, I.M., Abdelmalek, D.H., Elshahat, M.E., Elfiky, A.A., 2020. COVID-19 spike-host cell receptor GRP78 binding site prediction. J. Infect. 80, 554–562.

Isler, J.A., Skalet, A.H., Alwine, J.C., 2005. Human cytomegalovirus infection activates and regulates the unfolded protein response. J. Virol. 79, 6890–6899.

Janewanthanakul, S., Supungul, P., Tang, S., Tassanakajon, A., 2020. Heat shock protein 70 from *Litopenaeus vannamei* (LvHSP70) is involved in the innate immune response against white spot syndrome virus (WSSV) infection. Dev. Comp. Immunol. 102, 103476.

Jiang, S.G., Qiu, L.H., Zhou, F.L., Huang, J.H., Guo, Y.H., Yang, K., 2007. Molecular cloning and expression analysis of a heat shock protein (Hsp90) gene from black tiger shrimp (*Penaeus monodon*). Mol. Biol. Rep. 36, 127–134.

Jiang, Z.H., Zhang, K., Li, Z.L., Li, Z.G., Yang, M., Jin, X.J., Cao, Q., Wang, X.T., Yue, N., Li, D.W., et al., 2020. The *Barley stripe mosaic virus* γb protein promotes viral cell-to-cell movement by enhancing ATPase-mediated assembly of ribonucleoprotein movement complexes. PLoS Pathog. 16, e1008709.

Li, X.Y., Pang, L.R., Chen, Y.G., Weng, S.P., Yue, H.T., Zhang, Z.Z., Chen, Y.H., He, J.G., 2013. Activating transcription factor 4 and X box binding protein 1 of *Litopenaeus vannamei* transcriptional regulated white spot syndrome virus genes *wsv023* and *wsv083*. PLoS One 8, e62603.

Li, X.Y., Yue, H.T., Zhang, Z.Z., Bi, H.T., Chen, Y.G., Weng, S.P., Chan, S., He, J.G., Chen, Y.H., 2014. An activating transcription factor of *Litopenaeus vannamei* involved in WSSV genes *wsv059* and *wsv166* regulation. Fish Shellfish Immunol. 41, 147–155.

Li, C.Y., Wang, Y.J., Huang, S.W., Cheng, C.S., Wang, H.C., 2016. Replication of the shrimp virus WSSV depends on glutamate-driven anaplerosis. PLoS One 11, e0146902.

Li, H.Y., Wang, S., Chen, Y.G., Lǔ, K., Yin, B., Li, S.D., He, J.G., Li, C.Z., 2017. Identification of two p53 isoforms from *Litopenaeus vannamei* and their interaction with NF-κB to induce distinct immune response. Sci. Rep. 7, 45821.

Li, H.Y., Yin, B., Wang, S., Fu, Q.H., Xiao, B., Lǔ, K., He, J.G., Li, C.Z., 2018. RNAi screening identifies a new Toll from shrimp *Litopenaeus vannamei* that restricts WSSV infection through activating Dorsal to induce antimicrobial peptides. PLoS Pathog. 14, e1007109.

Li, C.Z., Weng, S.P., He, J.G., 2019. WSSV-host interaction: host response and immune evasion. Fish Shellfish Immunol. 84, 558–571.

Luan, W., Li, F.H., Zhang, J.Q., Wang, B., Xiang, J.H., 2009. Cloning and expression of glucose regulated protein 78 (GRP78) in *Fenneropenaeus chinensis*. Mol. Biol. Rep. 36, 289–298.

Luana, W., Li, F.H., Wang, B., Zhang, X.J., Liu, Y.C., Xiang, J.H., 2007. Molecular characteristics and expression analysis of calreticulin in Chinese shrimp *Fenneropenaeus chinensis*. Comp. Biochem. Phys. B Biochem. Mol. Biol. 147, 482–491.

Millard, R.S., Ellis, R.P., Bateman, K.S., Bickley, L.K., Tyler, C.R., van Aerle, R., Santos, E.M., 2021. How do abiotic environmental conditions influence shrimp susceptibility to disease? A critical analysis focussed on White Spot Disease. J. Invertebr. Pathol. 186, 107369.

Paskevicius, T., Farraj, R.A., Michalak, M., Agellon, L.B., 2023. Calnexin, more than just a molecular chaperone. Cells 12, 403.

Peña, J., Harris, E., 2011. Dengue virus modulates the unfolded protein response in a time-dependent manner. J. Biol. Chem. 286, 14226–14236.

Schröder, M., Kaufman, R.J., 2005. The mammalian unfolded protein response. Annu. Rev. Biochem. 74, 739–789.

Shen, J.S., Chen, X., Hendershot, L., Prywes, R., 2002. ER stress regulation of ATF6 localization by dissociation of BiP/GRP78 binding and unmasking of golgi localization signals. Dev. Cell 3, 99–111.

Shin, W.J., Ha, D.P., Machida, K., Lee, A.S., 2022. The stress-inducible ER chaperone GRP78/BiP is upregulated during SARS-CoV-2 infection and acts as a pro-viral protein. Nat. Commun. 13, 6551.

Siddique, M.A., Haque, M.I., Sanyal, S.K., Hossain, A., Nandi, S.P., Alam, A., Sultana, M., Hasan, M., Hossain, M.A., 2018. Circulatory white spot syndrome virus in South-West region of Bangladesh from 2014 to 2017: molecular characterization and genetic variation. Amb. Express 8, 25.

Stentiford, G.D., Neil, D.M., Peeler, E.J., Shields, J.D., Small, H.J., Flegel, T.W., Vlak, J.M., Jones, B., Morado, F., Moss, S., et al., 2012. Disease will limit future food supply from the global crustacean fishery and aquaculture sectors. J. Invertebr. Pathol. 110, 141–157.

Tassanakajon, A., Amparyup, P., Somboonwiwat, K., Supungul, P., 2011. Cationic antimicrobial peptides in penaeid shrimp. Mar. Biotechnol. 13, 639–657.

Umareddy, I., Pluquet, O., Wang, Q.Y., Vasudevan, S.G., Chevet, E., Gu, F., 2007. Dengue virus serotype infection specifies the activation of the unfolded protein response. Virol. J. 4, 91.

Van Etten, J., 2009. Lesser known large dsDNA viruses. Preface. Curr. Top. Microbiol. 328 (v–vii).

Walter, P., Ron, D., 2011. The unfolded protein response: from stress pathway to homeostatic regulation. Science 334, 1081–1086.

Wang, M., Kaufman, R.J., 2014. The impact of the endoplasmic reticulum protein-folding environment on cancer development. Nat. Rev. Cancer 14, 581–597.

Wang, S., Li, H.Y., Zhu, P., Fu, Q.H., Yin, B., Li, Q.Y., Chen, R.J., Jiang, X.W., Weng, S.P., He, J.G., et al., 2021. MAPKKK15 gene from shrimp *Litopenaeus vannamei* is transcribed in larva development stages and contributes to WSSV pathogenesis. Aquaculture 534, 736324.

Wang, C.Q., Wei, M.H., Wu, G.C., He, L.X., Zhu, J.H., Aweya, J.J., Chen, X.L., Zhao, Y.Z., Zhang, Y.L., Yao, D.F., 2022. Proteomics analysis reveals a critical role for the WSSV immediate-early protein IE1 in modulating the host prophenoloxidase system. Virulence 13, 936–948.

Xiao, B., Fu, Q.H., Niu, S.W., Zhu, P., He, J.G., Li, C.Z., 2020. Penaeidins restrict white spot syndrome virus infection by antagonizing the envelope proteins to block viral entry. Emerg. Microb. Infect. 9, 390–412.

Xu, J.X., Ruan, L.W., Shi, H., 2014. eIF2α of *Litopenaeus vannamei* involved in shrimp immune response to WSSV infection. Fish Shellfish Immunol. 40, 609–615.

Yan, D.C., Dong, S.L., Huang, J., Yu, X.M., Feng, M.Y., Liu, X.Y., 2004. White spot syndrome virus (WSSV) detected by PCR in rotifers and rotifer resting eggs from shrimp pond sediments. Dis. Aquat. Org. 59, 69–73.

Yu, C.Y., Hsu, Y.W., Liao, C.L., Lin, Y.L., 2006. Flavivirus infection activates the XBP1 pathway of the unfolded protein response to cope with endoplasmic reticulum stress. J. Virol. 80, 11868–11880.

Yuan, F.H., Chen, Y.G., Zhang, Z.Z., Yue, H.T., Bi, H.T., Yuan, K., Weng, S.P., He, J.G., Chen, Y.H., 2016. Down-regulation *apoptosis signal-regulating kinase 1* gene reduced the *Litopenaeus vannamei* hemocyte apoptosis in WSSV infection. Fish Shellfish Immunol. 50, 109–116.

Yuan, K., He, H.H., Zhang, C.Z., Li, X.Y., Weng, S.P., He, J.G., Chen, Y.H., 2017. *Litopenaeus vannamei* activating transcription factor 6 alpha gene involvement in ER-stress response and white spot symptom virus infection. Fish Shellfish Immunol. 70, 129–139.

Yuan, Z.Z., Chen, M., Wang, J.T., Li, Z.Y., Geng, X.Y., Sun, J.S., 2018. Identification of *Litopenaeus vannamei* BiP as a novel cellular attachment protein for white spot syndrome virus by using a biotinylation based affinity chromatography method. Fish Shellfish Immunol. 79, 130–139.